Chapter 4

Application of Vorticity Modeling to the Flow over 2-D Surface-Mounted Prism

Vorticity modeling is performed on a surface-mounted two-dimensional prism as shown in Fig. 4.1. In the schematic, the surface-mounting effects are simulated by having a mirror image of the flow around the prism. Obviously and from the geometry of the prism, it is expected that the flow will separate from the corners located at (0,h) and (1,h). The vorticity is then shed from the corners into the flow where it is free to undergo convection. With this simulation, we allow the vorticity created within the boundary layer to be shed into the flow. However, we do not take into consideration the effects of the vorticity generated in the boundary layer on any of the ground surfaces on the separation regions. The strengths of the vortices shed into the flow are determined by the boundary conditions on the surfaces of the prism, i.e., by the condition that there is no normal component of the velocity at the solid surface. To reduce the computational cost, the vortices are tracked for a downstream distance of four times the height of the prism. Unlike a grid-based method, no computation region needs to be defined for vorticity modeling as performed in this work.

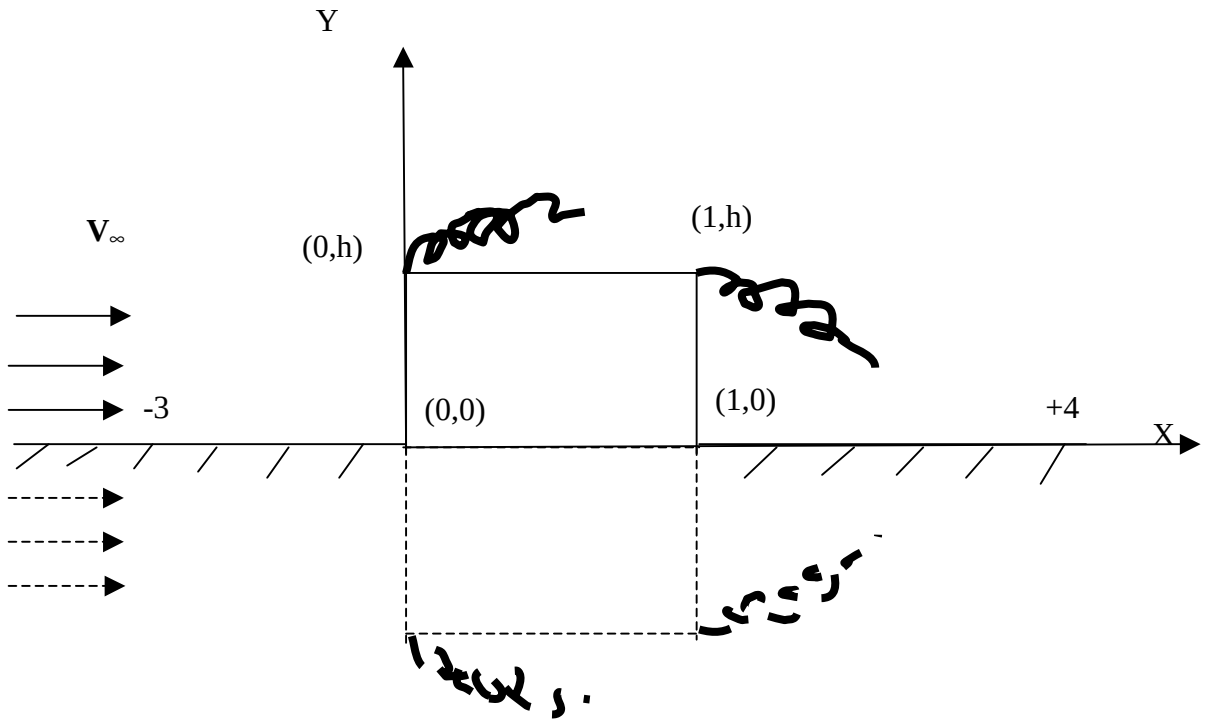

Fig. 4.1. Flow over surface-mounted 2-D prism

4.1 Vorticity surface model of the prism

The surfaces of the prism are modeled by vorticity elements as shown in Fig. 4.2. The vorticity elements in the mirror image have the same strength as in the actual flow, however, with opposite sign.

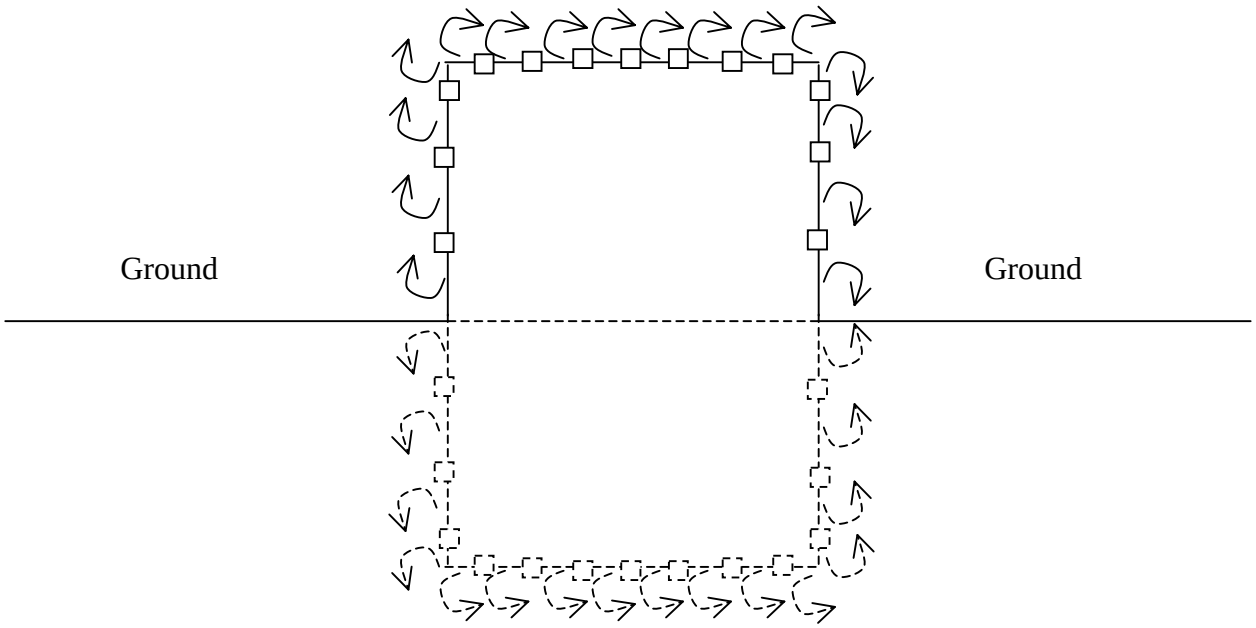

Fig. 4.2. Vorticity surface model for the prism

The two lateral surfaces are divided into elements of unequal lengths using the following generating function

$$Y_i = h * \sin[\frac{\pi}{2n}(i-1)] \qquad (4.1.1)$$

where n is the number of vorticity elements on the lateral surface, and Y_i is the y coordinate of node i. Equation (4.1.1) generates smaller elements as i approaches n. In other words, smaller elements are taken near the corners than near the ground. For the simulation presented here, n was set equal to 65. As for the top surface, elements with equal lengths are used. The length of each these elements on the top surface is set nearly equal to the length of the vorticity element

nearest to the corner at (0,h) on the left lateral surface. The midpoints of vorticity elements are selected as the control points.

The values of vorticity density, γ, at (0,0) and (1,0) are set equal to zero because of the symmetry caused by the image mirror system. Moreover, since vortex cores are introduced at the corners. the values of vorticity density over the panels covering these corners are also set equal to zero.

The boundary condition at the control points (x_c,y_c) is given by

$$(\vec{V}_b + \vec{V}_\infty + \vec{V}_w) \bullet \vec{n} = 0 \qquad (4.1.2)$$

where $\vec{n}$ is a vector normal to the vorticity sheet or surface of the prism. $\vec{V}_\infty$ is the velocity of the uniform stream, $\vec{V}_w$ is the velocity at (x_c,y_c) induced by the shed vortices based on an equation for a vortex blob to be introduced in the next section. $\vec{V}_b$ is the velocity component due to the vortex cores at the corners and the vortex elements over the surface of the prism. Thus, $\vec{V}_b$ is given by

$$\vec{V}_b = \sum_{i=1}^{N} \vec{V}_{bi} - \frac{1}{2\pi}\vec{e}_z \times \frac{\Gamma_{1t}(\vec{r} - \vec{r}_{1t})}{|\vec{r} - \vec{r}_{1t}|^2} - \frac{1}{2\pi}\vec{e}_z \times \frac{\Gamma_{2t}(\vec{r} - \vec{r}_{2t})}{|\vec{r} - \vec{r}_{2t}|^2} \qquad (4.1.3)$$

where $\vec{V}_{bi}$ is given by Equation (3.3.3.8), Γ_{1t} is the vortex strength at the upstream corner, Γ_{2t} is the vortex strength at the downstream corner, $\vec{r}_{1t}$ and $\vec{r}_{2t}$ are the position vectors. It should be also noted that $\vec{V}_b$ and $\vec{V}_w$ velocity vectors include the velocities from the vortices and vortex elements in the mirror image as well.

4.2 Discretization of convected vortices

Vorticity introduced at the corners located at (0,h) and (1,h) is convected with the flow. Ideally, this vorticity should be modeled as a continuous vortex sheet emanating from the corners. However, the sheet undergos wrapping, rolling and stretching, which presents a seeming discontinuity in the curvature. Consequently, this process is difficult to simulate with a continuous sheet (Rosenhead, 1931). Actually, the evolution of vortex sheets is accompanied by the problem of Kelvin-Helmholtz instability.

An alternative to introducing a continuous vortex sheet model is to introduce a system of point vortices [4]. Then, the total circulation resulting from these vortices, Γ_w, is the sum of the circulations around the individual vortices

$$\Gamma_w = \sum_{k=1}^{M} \Gamma_k \qquad (4.2.1)$$

where M is the number of vortices, and Γ_k is the circulation of vortex k.

One major problem with the system of point vortices arises when two vortices are convected close to each other. As a result of the singularity in the Biot-Savart law for the velocity field generated by a point vortex, the two vortices are convected very far apart at the next time step. This can be overcome by removing the singularity of point vortices using the concept of a vortex blob is introduced. The vortex blob distributes the vorticity of a point vortex over a small, but finite, circular core by means of a so-called core function

$$F(d) = \frac{d^2}{1+d^2} \qquad (4.2.2)$$

where

$$d = \frac{\left|\vec{r} - \vec{r}_k\right|}{\sigma} \qquad (4.2.3)$$

where σ is the small radius of the vortex blob, $\vec{r}$ represents the point in the flowfield where the velocity is being calculated, and $\vec{r}_k$ represents the point where the vortex blob is located. The velocity induced by these vortex blobs is then approximated by

$$\vec{V}_w(\vec{r},t) = -\frac{1}{2\pi}\vec{e}_z \times \sum_{k=1}^{M} \Gamma_k F(d) \frac{\vec{r} - \vec{r}_k}{\left|\vec{r} - \vec{r}_k\right|^2} \qquad (4.2.4)$$

$$= -\frac{1}{2\pi}\vec{e}_z \times \sum_{k=1}^{M} \Gamma_k \frac{\vec{r} - \vec{r}_k}{\left|\vec{r} - \vec{r}_k\right|^2 + \sigma^2}$$

In our work, we will introduce vortex blobs with σ set at 10^{-6} , nondimensionalized with the width of the prism. We introduce these vortices steadily at time intervals Δt of 0.006. This time interval was determined by trial and error. Smaller values for Δt resulted in the same flow. On the other hand, larger values for Δt such as 0.01 cause chaotic and irregular vortex convections.

4.3 Calculation of pressure on the surfaces of the 2-D prism

To obtain the pressure distribution on the surfaces, the Euler equation was integrated along the surface starting from (0,0). The Euler Equation is written as

$$\frac{\partial u_i}{\partial t} + \frac{\partial u_i u_j}{\partial x_j} = -\frac{1}{\rho}\frac{\partial p}{\partial x_i} \qquad (4.3.1)$$

The velocity at the solid surface is actually equal to the circulation per unit length γ. The reason being that the solid surface is taken as a vortex sheet of zero thickness with a velocity differential. When the vorticity is integrated across the vortex sheet, one obtains the circulation per unit length γ. The integrated form of the Euler equation is then written as

$$p(l) - p(0) = -\rho[\frac{d}{dt}\int_0^l \gamma dl + \frac{\gamma(l)^2 - \gamma(0)^2}{2}] \qquad (4.3.2)$$

where $p(0)$ is the pressure at the stagnation point (0,0) where zero velocity exists. $p(0)$ is obtained by integrating the Euler equation from -∞ to (0,0) along the x axis.

One major problem occurs when calculating the pressure at the two corners (0,h) and (1,h) where the velocities approach infinity due to the singularity in the Biot-Savart law. Accordingly, the values of pressure also approach negative infinity at the two corners, which is not realistic. To overcome this problem, pressures are not calculated at the two corners. Instead, pressures at points that are one vortex element away from the corners are calculated as shown in Fig. 4.3. For the left corner, the static pressure at point A, denoted as P_A, is calculated by integration from the far field. Because the static pressure is continuous across the corner, the static pressure at point B, denoted as P_B, is set equal to P_A. Integration is then performed between points B and C and the static pressure at point C, P_C, is calculated. By the same argument, the static pressure at point D, denoted as P_D, is then set equal to P_C [3].

The equations for calculating the pressure on the surface are summarized as follows.

For the left lateral surface, we write

$$p(l) - p(0) = -\rho[\frac{d}{dt}\int_0^l \gamma dl + \frac{\gamma(l)^2 - \gamma(0)^2}{2}] \qquad (4.3.3.a)$$

for the top surface, we write

$$p(l) - P_A = -\rho[\frac{d}{dt}\int_B^l \gamma dl + \frac{\gamma(l)^2 - \gamma(B)^2}{2}] \qquad (4.3.3.b)$$

and for the right lateral surface, write

$$p(l) - P_C = -\rho[\frac{d}{dt}\int_D^l \gamma dl + \frac{\gamma(l)^2 - \gamma(D)^2}{2}] \qquad (4.3.3.c)$$

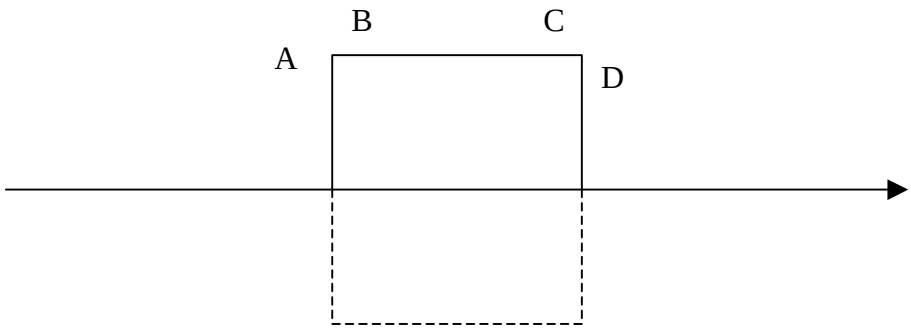

Fig. 4.3 Calculation of pressure

4.4 Numerical procedure

Since the values of γ at (0,0), (1,0), (0,h) and (1,h) are equal to zero, the number of unknowns is n-3+2, i.e., n-1, where n is the number of vorticity elements for the surfaces. Thus, the number of unknowns is one less than the number of equations, n. These equations are solved by the least square method.

The numerical procedure for the implementation of vorticity modeling as discussed above and as utilized in this work is summarized by the following steps:

1. The initial flow is specified. In the present case, a uniform stream with a velocity magnitude 1 is used. Vorticity elements and corner vortices of unknown strength are introduced.

2. Initial values for the circulation of the corner vortices Γ_{it} (i=1,2) and surface circulation γ are computed from the condition specified by equation (4.1.2).

3. The corner vortices are allowed to convect.

4. If desired, surface pressures are computed.

5. Once the vortices are allowed to convect and new corner vortices are introduced, new values of γ at the nodes and Γ_{it} (i=1,2) are computed from the condition specified by equation (4.1.2). The vortices in the wake are taken into account.

6. Time is advanced again and step 3 through 6 are repeated.

4.5 Parallelization of the computation

In general, the vorticity modeling method used here costs much less computer resources than grid-based methods such as DNS, LES. One issue with the vorticity modeling and the convection of the vortex blobs is that the information about the vortices should be kept for the computation for all time steps. Specifically, the positions and strengths of these vortices have to be tracked for every time step calculation. As the time advances, more vortices are introduced into the flow. As a result, more information needs to be kept and more calculations need to be conducted. Thus, the cost for the computation increases as the time advances. Another factor that affects the speed of computation is the number of vortex elements distributed over the surfaces of the prism. The speed for computation decreases when more vortex elements over the surfaces are introduced. We note that the most expensive part of the computation was the computation of the velocity induced by the surface vortex elements and the vortices in the flow. Since the velocity caused by each surface vortex element or each vortex blob in the flow can be calculated independently, and because the final flow is a mere superposition, this calculation can be parallelized. In our work, the parallelization was done on an SGI workstation with 8 processors and the computation was about 6 times faster than that without the parallelization.

4.6. Results

The magnitude of velocity, the vorticity in the flow field around a surface-mounted prism with a height to width ratio of 0.65, and the surface pressure distribution were calculated. The results are shown in Fig. 4.5 to Fig. 4.25.

4.6.1 Velocity magnitude

The velocity magnitude was calculated over a rectangular region that covers x from –1.0 to 2.0 and y from 0.0 to 1.95. Both x and y are nondimensionalized with the width of the prism. The contours of velocity magnitude from time steps between 21000 to 23000 with an interval of 100 time steps are shown in Fig 4.5 to 4.11. The magnitude of velocity is denoted by different colors. The black rectangle in the figures shows the prism.

As expected, low values for velocity magnitude always appear in the following three regions: (1) the separation region on the top surface, (2) the region near the stagnation points (0,0) and (1,0), and (3) part of the wake behind the prism. High values for velocity magnitude can be found outside the vorticity region in the upper part of the flow. It should be noted that the high values at the corners of the prism are caused by the singularity of Biot-Savart law that is used for the computation of the velocity field. Another feature to be noted is the outer edge of the shear layer where the magnitude of the velocity becomes around 0.95. It is shown by the light blue region over the separation. This edge has the same direction as the onset of separation. Further downstream, the shear layer shows variations. At times, the shear layer keeps on moving into the outer flow such as over observed time steps between 21200 and 21600. At other times, it curves back towards the prism as observed at times 21700 and 22600.

4.6.1 Vorticity

The vorticity field was calculated from the vorticity convected into the flow region around the prism. In order to ensure that the results presented are not dependent on the initial conditions, we show in Fig. 4.12 to 4.18 vorticity contours for time steps between 21000 to 23000 with an interval of 100 time steps. The strength of vorticity is denoted by different colors. The black rectangle in the figures shows the prism.

As shown in Fig 4.12 to Fig 4.18, vorticity is convected from the upstream corner in the flow region above the top surface of the prism and behind the rear surface, which is of course consistent with the real flow. As expected, this clockwise vorticity (denoted in this work as

positive) is shed along a sheet above the top surface. In all plots, we note a roll up of this sheet towards the middle of the prism. In a similar fashion, we note counter-clockwise vorticity forming at the dowstream corner as shown by the blue contours. This negative vorticity is caused by the upward velocity at the rear surface of the prism. It is interesting to note the interaction between the negative and positive vorticity. What seems to happen is that as the negative vorticity concentrates and become stronger, such as shown at time steps 21200 and 21300, there is an interaction between the opposite-sign vorticity regions whereby positive vorticity is pulled down and negative vorticity is lifted up as shown in time steps between 21400 and 21700. At time 21700 the shear layer curves back towards the prism. This is followed by the shedding of the negative vorticity into the flow as seen in time step 21800. It should be noted that the same process happens between time steps 21900 and 22500. This process is the major feature to be observed from the vorticity distribution.

4.6.2 Pressure

The pressure distribution over the front, top and rear surfaces of the prism was calculated from time step 21000 to time step 23000 with an interval of 100 time steps. Pressure coefficients corresponding to these distributions are shown in Fig. 4.19 to Fig 4.25. The pressure is normalized by $\rho V^2/2$, where ρ and V are both set equal to 1.0. The figures for the pressure coefficient are divided by the dashed lines into three regions that represent the pressure coefficient for the front surface, top surface, and rear surface respectively. The X-axis for these figures is an index number that corresponds to the points where pressure was calculated.

It is noted that the pressure coefficient at index number 1, which corresponds to the stagnation point (0,0), is almost 1.0 in all figures, as expected. The pressure decreases along the left surface and becomes negative when approaching the front corner. This is due to the increase in the speed of the flow at that location. Along the top surface, the pressure presents bigger variations near the rear corner. This is caused by the negative vorticity above the rear corner which forms at times and sheds at other times. On the rear surface, the pressure varies approximately between –0.5 and +0.5 from the rear corner to the point (1,0). These variations are due to the convection of vortices behind the rear surface.

4.6.3 Mean and rms values for pressure

Mean, rms(root mean square) and peak values of the pressure fluctuation for some locations on the top surface are shown in Fig. 4.26 to Fig. 4.29. The calculations were conducted at the points with index numbers 201 to 210, which corresponds to the region close to the front corner on the top surface. The x-coordinates in terms of the prism height for these points are shown in Table 4.1.

Table 4.1 x-location along the top surface for the points where mean and rms values for pressure are calculated

Index Number	x-location along the top surface
201	0.0077 h
202	0.0154 h
203	0.0231 h
204	0.0308 h
205	0.0385 h
206	0.0462 h
207	0.0539 h
208	0.0616 h
209	0.0693 h
210	0.0770 h

At the first location, i.e. x/h=0.0077, and for the time steps between 21000 and 23000 the pressure coefficient varied between peak values of –1.8 and a minimum value of almost –1.0. The mean value is –1.42 with an rms value of 0.31. These values are well within the range of values measured in smooth flows (Tieleman, 2001) [9]. For the other locations between x/h=0.015 and 0.08, the plots show a continuous decrease of the mean value from –1.2 at x/h=0.015 to –0.68 at x/h=0.08. For all locations, we note a peak value at time 22000 shown by index 11 on the plots. This peak value is about –1.5 at all locations.